IJC
International Journal of Cancer

The functional interlink between AR and MMP9/VEGF signaling axis is mediated through PIP5K1α/pAKT in prostate cancer

Per Larsson[1,2,3], Azharuddin Sajid Syed Khaja[3], Julius Semenas[3], Tianyan Wang[3], Martuza Sarwar[1], Nishtman Dizeyi[1], Athanasios Simoulis[4], Andreas Hedblom[1,3], Sun Nyunt Wai[3], Niels Ødum[2] and Jenny L. Persson[1,3]

[1]Division of Experimental Cancer Research, Department of Translational Medicine, Lund University, Clinical Research Centre, Malmö, Sweden
[2]Department of Immunology and Microbiology, University of Copenhagen, Copenhagen, Denmark
[3]Department of Molecular Biology, Umeå University, Umeå, Sweden
[4]Department of Clinical Pathology and Cytology, Skåne University Hospital, Malmö, Sweden

Currently, no effective targeted therapeutics exists for treatment of metastatic prostate cancer (PCa). Given that matrix metalloproteinases 9 (MMP9) and its associated vascular endothelial growth factor (VEGF) are critical for tumor vascularization and invasion under castration-resistant condition, it is therefore of great importance to define the functional association and interplay between androgen receptor (AR) and MMP9 and their associated key survival and invasion pathways in PCa cells. Here, we found that there was a significant correlation between MMP9 and AR protein expression in primary and metastatic PCa tissues, and a trend that high level of MMP9 expression was associated with poor prognosis. We demonstrated that constitutive activation of AR increased expression of MMP9 and VEGF/VEGF receptors. We further showed that AR exerts its effect on MMP9/VEGF signaling axis through PIP5K1α/AKT. We showed that MMP9 physically interacted with PIP5K1α *via* formation of protein–protein complexes. Furthermore, elevated expression of MMP9 enhanced ability of AR to activate its target gene cyclin A1. The elevated sequential activation of AR/PIP5K1α/AKT/MMP9/VEGF signaling axis contributed to increased invasiveness and growth of metastatic tumors. Conversely, treatment with PIP5K1α inhibitor significantly suppressed invasiveness of PCa cells expressing constitutively activated AR, this was coincident with its inhibitory effect of this inhibitor on AR/MMP9/VEGF pathways. Our results suggest that AR and MMP9-associated network proteins may be effectively targeted by blocking PIP5K1α/AKT pathways using PIP5K1α inhibitor in metastatic PCa.

Introduction

During the development of advanced prostate cancer (PCa), in particular, castration-resistant PCa (CRPC), elevated level of androgen receptor (AR) is necessary and sufficient to confer androgen-sensitive cells to invasive and castration-resistant phenotypes.[1–4] *AR* gene amplification, protein stabilization and duplication of *AR* gene enhancer are some of the mechanisms underlying AR overexpression.[2,3] *AR* enhancer duplication was recently reported to be associated with inactivated tumor suppressor *PTEN*, a negative regulator of PI3K/AKT pathways.[3,4]

Additional Supporting Information may be found in the online version of this article.

Key words: matrix metalloproteinases 9, PIP5K1α, AKT, androgen receptor, metastatic prostate cancer, targeted therapy

Abbreviations: AR: androgen receptor; DHT: dihydrotestosterone; DSF: disease-free survival; MMP9: matrix metalloproteinase 9; PCa: prostate cancer; PIP5K1α: phosphatidylinositol 4-phosphate 5-kinase type-1 alpha; VEGF: vascular endothelial growth factor

Conflict of interest: No conflict of interest.

Grant sponsor: Barncancerfonden; **Grant number:** TJ2015-0097; **Grant sponsor:** Cancerfonden; **Grant number:** 170621; **Grant sponsor:** H2020 Marie Skłodowska-Curie Actions; **Grant number:** 721297; **Grant sponsor:** Kempestiftelserna; **Grant sponsor:** Norland fund for Cancer Forskning, Umeå University; **Grant sponsor:** Swedish Foundation for International Cooperation in Research and Higher Education; **Grant number:** IG2013-5595; **Grant sponsor:** Government Health Innovation Grant; **Grant sponsor:** The Royal Physiographical Foundation; **Grant sponsor:** Umeå University, Medical Faculty Grants

DOI: 10.1002/ijc.32607

History: Received 20 Feb 2019; Accepted 25 Jul 2019; Online 5 Aug 2019

Correspondence to: Jenny L. Persson, Department of Molecular Biology, Umeå University, 901 87 Umeå, Umeå, Sweden and Division of Experimental Cancer Research, Department of Translational Medicine, Lund University, Clinical Research Center, Jan Waldenströms gatan 35, 205 02 Malmö, Sweden, Tel.: +46-0706-391106, E-mail: jenny_l.persson@med.lu.se; jenny.persson@umu.se

What's new?

The androgen receptor (AR) is a key factor in prostate cancer (PCa) progression and metastasis. Given that matrix metalloproteinase 9 (MMP9) and the vascular endothelial growth factor (VEGF) pathway are critical for tumor vascularization and invasion under castration-resistant condition, it may be of importance to define the functional interplay between AR and MMP9 and their associated key survival and invasion pathways in PCa cells. This study identifies novel cooperative mechanisms involving AR, the MMP9/ VEGF signaling axis and PIP5K1α/AKT pathways driving tumor invasion. The findings provide new information to guide the development of targeted therapy for invasive castration-resistant prostate cancer.

Altered expression of coactivators of AR is another mechanism that affects AR signaling by inducing abnormal transactivation of their target genes to enable increased survival and invasiveness of PCa.[2] Thus, AR-dependent mechanisms, including constitutively active or inappropriately restored of AR, or indirect AR activation by growth factors and cytokines in the castration or androgen-depleted environment, highlight a common feature of CRPC which is addiction to AR-associated signaling.[5]

Phosphatidylinositol 4-phosphate 5-kinase type-1 alpha (PIP5K1α) is a dominant lipid kinase that is responsible for producing PI(4,5)P2, also termed PIP2.[6,7] PIP2 is a lipid substrate used by phosphatidylinositol 3-kinase (PI3K) to produce phosphatidylinositol 3,4,5-trisphosphate (PIP3) for the activation of AKT family of serine/threonine kinases.[6–8] PIP5K1α is thereby a key lipid kinase that acts on upstream of PI3K/AKT pathways. Alterations in AKT pathways are the most frequent events observed in various types of metastatic cancer.[9] Only until recent years, owing to the discovery of new cancer biomarkers, an important role of PIP5K1α in cancer metastasis has been identified.[10,11] We, for the first time, showed that altered PIP5K1α expression significantly correlated with alterations in PI3K/AKT/PTEN pathways and was associated with poor prognosis in PCa patients.[10] Amplification of the gene encoding for PIP5K1α is a frequent event in breast cancer.[11] Our recent studies further provide evidence suggesting that PIP5K1α is a key player in the development of triple-negative breast cancer.[12] Overexpression of PIP5K1α promoted tumor growth and invasiveness by increasing activity of PI3K/AKT in mouse xenograft models.[12,13]

It is well-established that matrix metalloproteinase 9 (MMP9) is involved in degradation of ECM and vascular remodeling during tumor cell invasion.[14] It has been shown that MMP9 expression is regulated by epidermal growth factor receptor (EGFR) *via* PI3K/AKT pathways in cancers of the lung, ovary and breast.[15–18] EGFR is also up-regulated in MMP9 overexpressing PCa cells, which suggests that MMP9 is also associated with EGFR pathways in PCa.[19] It has been shown that MMP9 regulates vascular endothelial growth factor (VEGF) signaling axis by cleaving membrane-bound VEGF, leading to the increased bioavailability for its receptor VEGFR2.[20] Thus, MMP9 may amplify local angiogenesis due to its ability to elevating the level of VEGF in tumors.[21] MMPs have considered as intriguing targets for therapeutic intervention for treatment of metastatic PCa. Various types of MMP inhibitors have been tested in several clinical trials, but failed to increase patient survivals, probably due to the lack of specificity and selectivity of these inhibitors.[22] Given that the current understanding of MMP9 in cancer progression and metastasis mainly comes from its role in tumor-associated microenvironment,[22] there is an unmet need to define the pathways that are associated with MMP9 and the role of intracellular MMP9 in PCa cells.

There are unmet needs for novel therapeutic agents that can effectively target and inhibit AR signaling pathways in metastatic PCa. Several novel approaches to inhibit interactions between coregulators and AR by using peptidomimetics have been tested in PCa cell lines and xenograft mice and showed promising effects.[23] We have discovered a selective PIP5K1α inhibitor, ISA-2011B, which blocks PI3K and its downstream AKT phosphorylation at Serine 473 (pAKT S473) pathway through inhibition of PIP5K1α in PCa cells.[12,13] Treatment with ISA-2011B suppressed growth and invasion of PCa in xenograft mice.[10,12,13] Interestingly, ISA-2011B treatment abolished AR expression by inducing degradation of AR, as PIP5K1α mediates AR stabilization in PCa cells.[13]

In our study, we investigated the clinical importance of MMP9 and its association with AR in primary and metastatic tissues from PCa patients. We further unrevealed molecular mechanisms underlying the interconnected pathways of AR, MMP9/VEGF and PIP5K1α/AKT in PCa cell lines and in tumor xenograft mouse model. Our results suggest that AR and MMP9-associated network proteins may be effectively targeted by blocking PIP5K1α/AKT pathways in CRPC and metastatic PCa.

Materials and Methods

Tissue specimens, tissue microarrays and mRNA expression data

Tissue microarrays (TMAs) containing primary PCa (n = 17) and metastatic PCa lesions in distant organs such as lymph node, lung, liver and bone (n = 43) from 14 PCa patients, and benign prostatic hyperplasia (BPH; n = 48) *vs*. matched PCa tissues (n = 48) from 48 patients were constructed at Department of Clinical Pathology and Cytology, Skåne University Hospital, Malmö.[10] For mRNA expression and copy number alteration (CNA) data for MMP9, the disease-free survival (DFS) data were extracted from the open-access cBioPortal databases. MSKCC Prostate Oncogenenome Project dataset (for primary tumors, n = 181; for metastatic tumors n = 37) as described.[10,13] The follow-up time from diagnosis to disease recurrence known as biochemical recurrence (BCR) ranged

from 1 to 60 months was used for analysis of DFS. The study was approved by the Ethics Committee, Region Skåne, and Ethics Committee, Umeå Region and the Helsinki Declaration of Human Rights was strictly observed.

Immunohistochemical analysis

Immunohistochemistry on tumor tissue microarrays (TMA) was performed as previously described.[13] The staining of the tumor tissue was performed by using a semiautomatic staining machine (Ventana Inc, Tuscon, AZ). The specimens from the tumor tissues were evaluated and scored by four different scientists, including a pathologist. The stained slides were scored based on the staining intensity, as 0 (negative), 1 (weakly positive), 2 (moderately positive), 3 (strongly or very strongly positive) by using an arbitrary semiquantitative scale.

Cell culture and treatments

VCaP (RRID:CVCL_2235), PC-3 (RRID:CVCL_0035) and U-937 cells (RRID:CVCL_0007) were purchased from American Type Culture Collection (ATCC, Manassas, VA). All human cell lines have been authenticated using STR profiling within the last 3 years. All experiments were performed with mycoplasma-free cells. For treatment with dihydrotestosterone (DHT), medium containing 10% charcoal-stripped serum and 5 nM DHT or vehicle control 0.1% dimethyl sulfoxide (DMSO, Sigma-Aldrich, St. Louis, MO) were used. PIP5K1 alpha inhibitor: ISA-2011B, a diketopiperazine fused C-1 indol-3-yl substituted 1,2,3,4-tetrahydroisoquinoline derivative, ISA-2011B[10] at a final concentration of 50 μM in 1% DMSO was used for treatment for 48 hr.

Immunoblot, immunoprecipitation analysis and subcellular fractionation

Subcellular fractionation, immunoblot and immunoprecipitation analysis were performed as described previously.[10] Briefly, protein from different subcellular fractions (cytoplasmic and nuclear) was isolated by using NE-PER™ Nuclear and Cytoplasmic Extraction Reagents according to manufacturer's protocol (Thermo Fischer Scientific, Sweden). Signals were visualized and documented with an AlphaImager CCD system. Densitometric quantification of immunoblots was performed by the ImageJ Image Analysis Software (NIH, Baltimore, MD) and represented as fold change relative to control and was normalized relative to actin or GAPDH bands. For immunoprecipitation analysis, antibody against PIP5K1α was used to pull down the immune-complexes, and antibody to IgG (Thermo Fischer Scientific, Sweden) was used as a negative control.

Immunofluorescence analysis

PCa cells were seeded on glass coverslips and were subsequently treated with the different agents. Cells were fixed with 4% paraformaldehyde in PBS. For blocking background staining from nonspecific interactions, Image-iT™ FX signal enhancer (Molecular Probes, Inc, Eugene, OR) was used. The secondary antibodies including rabbit antidonkey conjugated to Rhodamine or Alexa Fluor 555 (Chemicon/Millipore International Inc, Temecula, CA) or antigoat conjugated to FITC antibodies and goat antirabbit Alexa Fluor 488 (Invitrogen, Stockholm, Sweden) were used. 4′,6-Diamidino-2-phenylindole counterstain (SERVA Electrophoresis GmbH, Heidelberg, Germany) was used to visualize cell nuclei. The images were viewed and taken under an Olympus AX70 fluorescent microscope or a Nikon Eclipse 90i Confocal microscope (Nikon DS-U1) and software ACT2U (ACT2U version. 1.5, Stockholm, Sweden) was used.

Plasmids and transfection

For transient transfection experiment, we used pCMV empty vector and pCVM vector containing full-length AR. For induction of MMP9 overexpression into the PCa cells, PLX-304 empty vector and PLX-304-MMP9 vector were used. TransIT-2020 kit (Mirus Bio, MIR5410, Madison, WI) was used by following the manufacturer's protocol.

Luciferase assays

PC-3 cells were transiently transfected with different vectors along with the reporter vector containing luciferase gene (Luc) or full-length cyclin A1 promoter in Luc reporter vector (cyclin A1-Luc) as indicated. The dual luciferase reporter assay kit was used according to the manufactures instructions (Promega, Madison, WI). The Firefly Luciferase and Renilla Luciferase activity were determined by using an Infinite® M200 multimode microplate reader (Tecan Sunrise™), equipped with dual injector.

Migration assay

Cell migration assays were performed using Transparent PET Membrane chambers (Corning, Germany). A total of $0.5–2 \times 10^5$ cells in RPMI 1640 phenol red-free and serum-free medium were seeded in the upper chamber, and 50% FBS as a chemoattractant was loaded in the lower chamber to allow the migration to proceed for 18 hr. For examination of the migratory ability of the tumor spheroids, 30 spheroids (each spheroid consists of approximately 100 cells) from each group were subjected to the migration assay. The migrated cells were counted and microphotographs were taken under Nikon Eclipse microscope.

RNA purification and quantitative RT-PCR

mRNA was purified from VCaP cells after treatment. The following primers were used in PCR: PIP5K1α forward: 5′-AGA TTC CCT GCG TTC ACC TT-3′, reverse: 5′-TGA GGC TTT GCG CTT AAT GG-3′. GAPDH forward: 5′-AAC AGC GAC ACC CAC TCC TC-3′, reverse: 5′-GGA GGG GAG ATT CAG TGT GGT-3′. PCR was performed under the following cycling condition: DNA denaturation for 30 sec at 98°C, 18 cycles of 30 sec annealing at 65.5°C and 30 sec extension at 72°C, and final 10 min extension at 70°C. Semiquantification

was performed using ImageJ Image Analysis Software (NIH, Bethesda, MD).

Tumor-spheroid formation assays

About 5×10^3 single cell suspension were cultured in suspension in modified spheroid medium containing DMEM F-12, 3.151 g/l Glucose, L-Glutamine (Lonza, Morristown, NJ), 2x B27 (Thermo Fisher Scientific, Waltham, MA), 20 ng/ml EGF (Sigma-Aldrich) and 20 ng/ml FGFβ (Sigma-Aldrich). For tumor-spheroid formation assays from the PCa cells stimulated with U-937 cells, monocultures or PCa cells after stimulation with U-937 cells were made in single cell suspensions, 1×10^5 PCa cells or 2×10^5 U937 cells were subjected to the tumor-spheroid formation assays in modified spheroid medium for 10–14 days and then counted

Mouse model of PCa derived from tumor spheroids stimulated by myeloid cells

The animal studies were approved by the Swedish Regional Ethical Animal Welfare Committee. The animal welfare and guidelines were strictly followed. Athymic NMRI nude male mice (Charles River Biotechnology, Wilmington, MA) aged 6 weeks and weighing 25–29 g were used. Equal amount of single-cell suspension from 1,000 tumor-spheroids derived from pLX304-MMP9 or control transfected-VCaP cells prestimulated with U-937 cells was injected subcutaneously into mice (n = 5 mice/group). To assess the luciferase live-imaging, luciferin was injected into each mice 5–10 min before imaging. The *in vivo* imaging device (IVIS imaging system, PerkinElmer, MA) was used.

Statistical analysis

For statistical analysis, Student's t-test and Spearman rank correlation tests were performed by using the Statistical software, Social Sciences software (SPSS, version 21, Chicago, IL). All outcome variables are representative of at least three independent experiments. All statistical tests performed were two-sided and p-value < 0.05 considered as statistical significant.

Data availability

The data that support the findings of our study are available from the corresponding author upon reasonable request.

Results

Expression of correlation between AR and MMP9 in bone metastasis in patient tissue

MMP9 is known to promote cancer invasion and metastasis.[22] However, it remained unclear whether MMP9 expression might be correlated with AR expression and patient outcome in primary and metastatic tissues from PCa patients. We performed immunohistochemical analysis to examine expression AR and MMP9 on TMAs previously constructed to contain primary tumor tissues and metastatic lesions from PCa patient cohorts.[24] Expression of AR was detected in both cytoplasmic and nuclear compartments in cancer cells (Fig. 1*a*). Expression of AR was significantly higher in metastatic lesions including lymph node, lung, liver and bone/bone marrow compared to that of the primary PCa tissues ($p < 0.001$; Fig. 1*b*). MMP9 expression was observed predominantly in cancer cells from the primary and metastatic tissues (Fig. 1*c*). MMP9 expression was higher in primary PCa tissues which expressed high level of AR than those expressed low level of AR, and this was statistically significant ($p < 0.001$; Fig. 1*d*). Spearman-rank correlation test revealed that there was a significantly positive correlation between AR and MMP9 protein expression ($r^2 = 0.405$, $p < 0.001$) in PCa tissues from this patient cohort.

We next examined MMP9 mRNA expression in primary tumor tissues (n = 150) from a patient cohort by using MSKCC Prostate Oncogenome Project publicly available at cBioPortal Database.[25] MMP9 mRNA expression was not statistically significantly higher in metastatic tissues compared to the primary PCa tissues. Furthermore, there was no statistically significant correlation between MMP9 and AR at mRNA levels. Next, we performed Kaplan–Meier survival analysis. We observed that there was a trend that patients with higher level of MMP9 mRNA expression (n = 127) suffered poorer DFS as compared to those with lower level (n = 13), but this difference was not statistically significant (p = 0.078; Fig. 1*e*). Further, alterations, in particular, amplification in *MMP9* gene were detected in 11% of PCa cases (n = 150) from the MSKCC Prostate cBioPortal Database (Fig. 1*f*). These data suggested that patients with higher level of MMP9 mRNA expression may suffer cancer metastasis and poor outcome.

The link among AR, PIP5K1α and MMP9 pathways in VCaP cells

Next, we wanted to investigate whether elevated levels of AR and MMP9 expression in tumor tissues from PCa patients might be related to their roles in promoting PCa invasion and metastasis. To this end, we firstly examined the effect of AR overexpression on MMP9 protein level in VCaP cells, a castration-resistant PCa cell line. Overexpression of AR was induced into VCaP cells by transfecting the cells with pCMV-AR or pCMV control vectors, followed by the treatment of cells with DHT at 5 nM to further stimulate activation of AR. AR expression was significantly increased in VCaP cells transfected with pCMV-AR compared to that of the control ($p < 0.001$; Fig. 2*a*). Significantly, DHT also increased expression of endogenous AR and transfected AR in VCaP cells compared to that of the controls ($p < 0.001$; Fig. 2*a*), suggesting that ligand binding of AR-enhanced its protein expression. Furthermore, AR expression was predominantly nuclear in VCaP cells transfected with control pCMV vector and was markedly enhanced in AR-transfected or DHT-stimulated cells as determined by immunofluorescence analysis (Fig. 2*b*). We next examined the effect of induced AR overexpression and DHT stimulation on MMP9 expression. Interestingly, overexpression of AR resulted in a significant

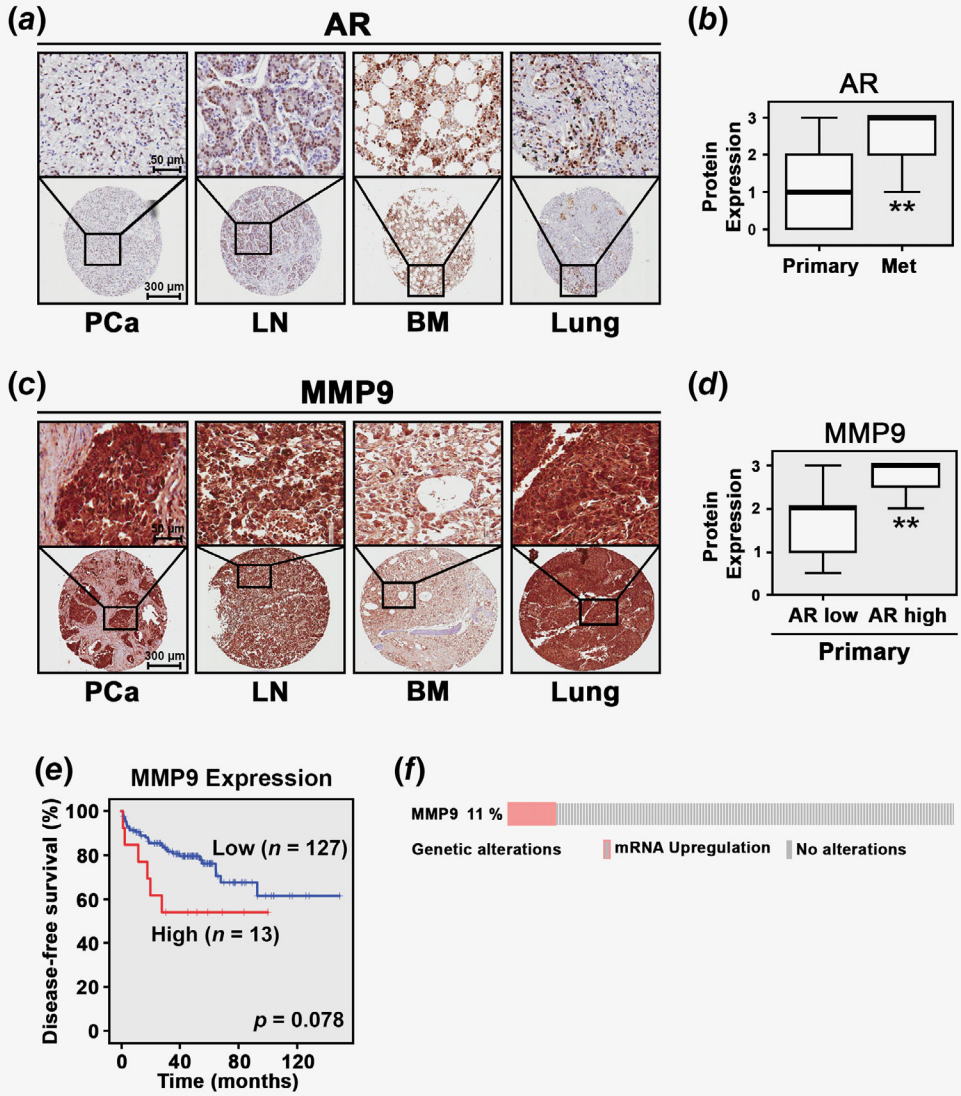

Figure 1. Correlation between the expression of MMP9 and AR at protein and mRNA levels in primary cancer tissues and metastatic lesions with patient outcome. (*a*) Representative microphotographs of immunohistochemical analysis of AR expression in tissue microarrays (TMA) containing PCa specimens and metastatic lesions in lymph node (LN), bone marrow (BM) and lung from PCa patients. The sections of tissues were analyzed with Olympus BX51 microscope at 20× or 40× magnification and microphotographs were taken by using a high-resolution scanner (ScanscopeCS, Aperio, Vista, CA). (*b*) Box-plot quantitative comparison of AR protein expression in primary *vs*. metastatic tissues ($p < 0.001$) is shown. (*c*) Representative microphotographs of MMP9 in various types of tissues as shown in (*a*). (*d*) Box-plot quantitative comparison of MMP9 protein expression in AR low *vs*. AR high primary tumors ($p < 0.001$). Paired Wilcoxon's rank sum test analysis is used. Scale bars are indicated and applied to all images in the panel. (*e*) Kaplan–Meier survival analysis based on BCR-free survival shows the difference between patients with low and high expression of MMP9. Differences in BCR-free survival between the two groups were calculated using the log-rank test ($p = 0.078$). (*f*) Alterations (11%) in MMP9 gene in PCa cancer tissues are shown.

increase in MMP9 expression by approximately 24% of the control (mean values of MMP9 expression in pCMV control cells and pCMV-AR cells were 0.62 and 0.72, difference = 0.1, 95% CI = 0.70–0.74, $p = 0.008$; Fig. 2*c*). DHT treatment also significantly enhanced MMP9 expression (mean MMP9 in pCMV control cells and DHT-treated pCMV cells were 0.62 and 0.71, difference = 0.09, 95% CI = 0.69–0.73, $p = 0.03$; Fig. 2*c*), suggesting that AR affects MMP9 expression in VCaP cells. We have previously shown that lipid kinase PIP5K1α acts as cofactor of AR by forming protein–protein complexes with AR in PCa cells,[10,13] and PIP5K1α/pAKT is also functionally associated with MMP9. We therefore examined whether AR overexpression might also affect PIP5K1α/pAKT in VCaP cells. Significantly, AR overexpression resulted in increased PIP5K1α compared to the control ($p < 0.001$; Fig. 2*d*). Interestingly, DHT stimulation also led to a significant increase in PIP5K1α protein level ($p = 0.002$; Fig. 2*d*). Similarly, expression of phosphor-475 AKT, the downstream effector of PIP5K1α was

remarkably increased in AR-transfected cells ($p = 0.009$) and in DHT-stimulated cells as well ($p = 0.03$; Fig. 2*d*). In agreement with our previous studies,[10,12,13] our findings here provided new evidence suggesting that AR, MMP9 and PIP5K1α/AKT may be interconnected with each other in PCa cells.

Given that VEGF is a growth factor critical for tumor vascularization and invasion under castration-resistant condition, and it is functionally related to MMP9, we wanted to examine whether AR overexpression might have impact on VEGF-associated angiogenic signaling. Indeed, expression of VEGF was significantly increased in VCaP cells overexpressing AR compared to that of the control (mean values of VEGF expression in pCMV control and pCMV-AR cells were 0.65 and 0.97, difference = 0.32, 95% CI = 0.95–0.98, $p = 0.002$), and in VCaP cells treated with DHT compared to cells treated with DMSO control (mean expression of VEGF expression in pCMV

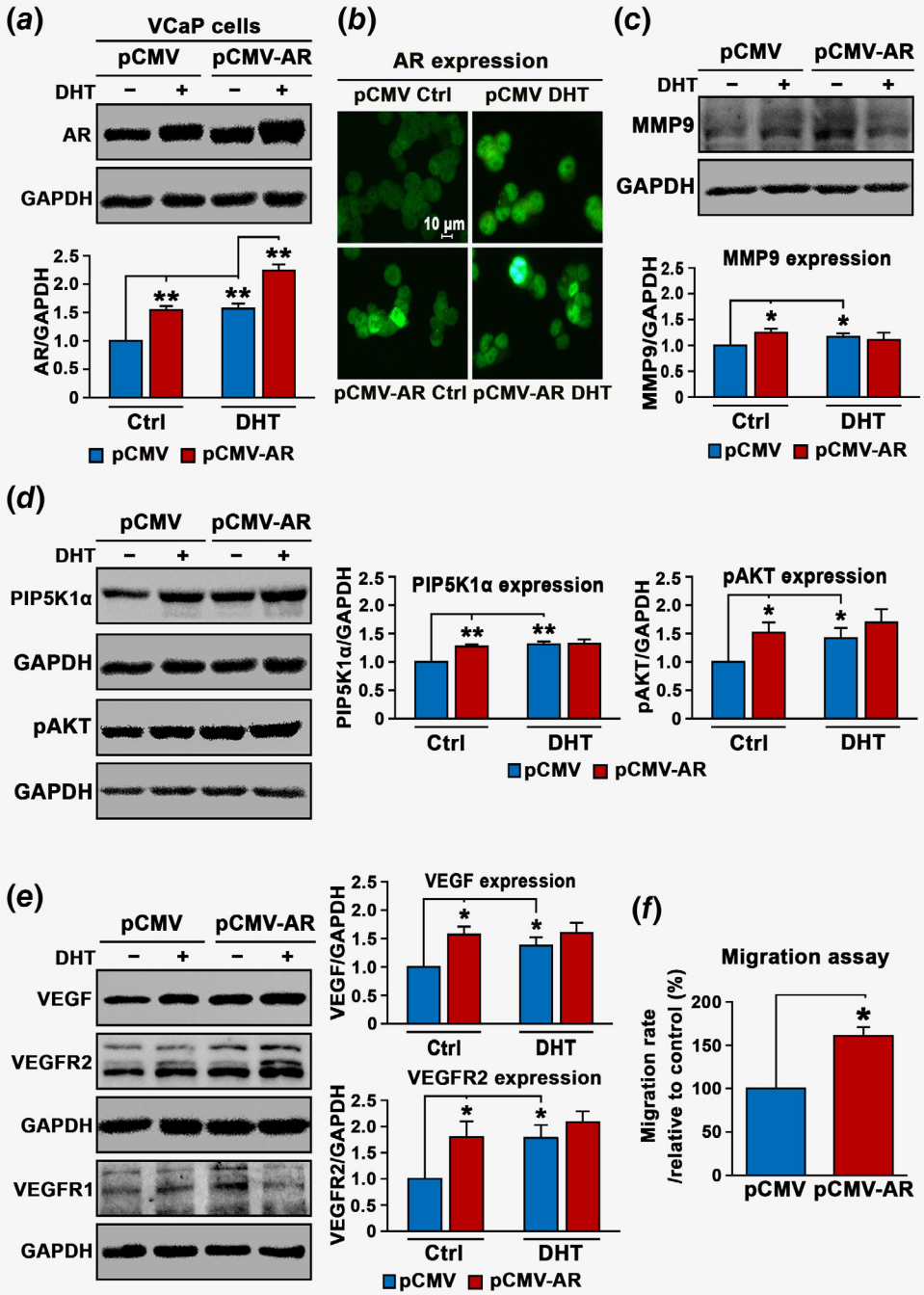

Figure 2. Legend on next page.

control and DHT-treated pCMV cells were 0.65 and 0.87, difference = 0.21, 95% CI = 0.84–0.89, $p = 0.023$; Fig. 2*e*). The similar effects of AR overexpression and DHT-stimulation on VEGFR2 were observed (mean expression of VEGFR2 in pCMV control and pCMV-AR cells were 0.4 and 0.69, 95% CI = 0.64–0.73, difference = 0.29, $p = 0.024$; mean expression of VEGFR2 in pCMV control and in DHT-treated pCMV cells were 0.4 and 0.72, difference = 0.32, 95% CI = 0.66–0.78, $p = 0.01$; Fig. 2*e*). AR overexpression increased expression of VEGFR1 (mean expression of VEGFR1 in pCMV control and pCMV-AR cells were 0.31 and 0.45, difference = 0.14, 95% CI = 0.45–0.46, $p < 0.001$), whereas DHT had no significant effect on VEGFR1 (Fig. 2*e* and Supporting Information Fig. S1).

Next, we wanted to elucidate the functional effect of AR on the behavior of VCaP cells. We observed that AR overexpression increased migratory ability of VCaP cells by 60% as compared to controls ($p = 0.004$, Fig. 2*f*). This suggests that AR-induced cascades of proteins MMP9, PIP5K1α/pAKT and VEGF signaling axis may have functional impact on the invasive behaviors of VCaP cells.

The functional link between AR and MMP9 is mediated by PIP5K1α

We hypothesize that AR may recruit PIP5K1α as a coregulatory protein to the AR complexes to trigger the activation of downstream pathways. To this end, we examined the effect of depletion of PIP5K1α from AR complexes on AR, pAKT, MMP9 and VEGF signaling axis in VCaP cells. Consistent with previous studies in PC-3 and LNCaP cells,[10,13,19] PIP5K1α was inhibited by using its inhibitor ISA-2011B, which led to a significant down-regulation in PIP5K1α and phosphorylated AKT (for PIP5K1α, $p = 0.003$; for pAKT, $p < 0.001$; Figs. 3*a* and 3*b*). Treatment of VCaP cells with ISA-2011B resulted in decreased AR expression in VCaP cells ($p < 0.001$; Fig. 3*a*), also in agreement with our previous studies.[10,13,19] Immunofluorescence analysis further revealed that ISA-2011B treatment remarkably reduced PIP5K1α in both cytoplasm and nucleus, which was accompanied with the reduced tubulin staining signals and disrupted membrane structure as well as the nuclear intensity of AR in VCaP cells (Figs. 3*c* and 3*d*). Similar inhibitory effects of ISA-2011B on MMP9 expression was observed (mean value of MMP9 expression in vehicle control and in ISA-2011B-treated cells were 2.32 and 1.23, difference = 1.09, 95% CI = 0.94–1.53; $p < 0.001$; Fig. 3*e*). The membrane/cytosolic expression of MMP9 was remarkably reduced in VCaP cells treated with ISA-2011B as determined by immunofluorescence analysis (Fig. 3*f*). Next, we examined whether PIP5K1α and MMP9 may be physically interact with each other in the subcellular compartments. To this end, we fractionated VCaP cells into membrane/cytoplasmic and nuclear fractions. The immunoprecipitation assays were performed by using lysates of membrane/cytoplasmic and nuclear fractions. We observed the presence of MMP9 in the PIP5K1α-associated protein-complexes predominantly in the membrane/cytosol compartments of VCaP cells (Fig. 3*g*). Immunofluorescence analysis of the double costained cells with antibodies against PIP5K1α (red) and MMP9 (green) under confocal microscope further confirmed the colocalization of PIP5K1α and MMP9 predominantly in the membrane/cytosol compartments of VCaP cells (orange; Fig. 3*h*). These findings suggest that MMP9 may physically interact with PIP5K1α to mediate the downstream signaling.

We next examined the effect of blocking PIP5K1α on VEGF signaling axis. ISA-2011B treatment efficiently blocked VEGF expression (mean value of VEGF expression in vehicle control and in ISA-2011B-treated cells were 0.71 and 0.45, difference = 0.26, 95% CI = 0.42–0.47; $p < 0.001$, Figs. 4*a* and 4*b*). Similarly, ISA-2011B treatment also led to a significant decrease in the expression of VEGFR1 (mean value of VEGFR1

Figure 2. The interplay between AR and MMP9 and PIP5K1α in VCaP cells. (*a*) Immunoblots show the expression of AR in control (0.1% DMSO) treated or DHT treated VCaP cells expressing either control (pCMV) or AR expressing vectors (pCMV-AR). Data is presented as average of three independent experiments (mean values of AR expression in control pCMV cells and pCMV-AR cells was 0.70 and 1.03, difference = 0.33, 95% CI = 1.01–1.06, $p < 0.001$; Mean AR expression in control pCMV cells and DHT-treated pCMV cells was 0.70 and 1.04, difference = 0.34, 95% CI = 1.02–1.06, $p < 0.001$; Mean AR expression in control pCMV cells and in DHT-treated pCMV-AR cells was 0.70 and 1.5, difference = 0.80, 95% CI = 1.44–1.55, $p < 0.001$). (*b*) Representative immunofluorescent images show the expression and subcellular localization of AR in VCaP cells overexpressing AR or control vector that were treated with DMSO or DHT. (*c*) Immunoblots show the expression of MMP9 in either control or DHT treated VCaP cells expressing pCMV or pCMV-AR vectors ($p = 0.008$ *vs.* $p = 0.03$). (*d*, *e*). Immunoblots show the expression of PIP5K1α and pAKT S473 in (mean values of PIP5K1α expression in pCMV control cells and in pCMV-AR cells were = 0.66 and 0.85, difference = 0.19, 95% CI = 0.84–0.85, $p < 0.001$; Mean PIP5K1α expression in pCMV control cells and in DHT-treated pCMV cells were = 0.66 and 0.88, difference = 0.22, 95% CI = 0.87–0.88; $p = 0.002$). PIP5K1α was detected on the same gel/membrane as for AR, and they share the same GAPDH as a loading control. Mean value of pAKT expression in pCMV control cells and in pCMV-AR cells were 0.85 and 1.15, difference = 0.3, $p = 0.009$; Mean value of pAKT expression in pCMV control cells and in DHT-treated pCMV cells were 0.85 and 1.06, difference = 0.21, 95% CI = 1.02–1.09, $p = 0.03$), and for VEGF, VEGFR1 and VEGFR2 (for VEGF expression, $p = 0.002$; VEGF expression in DHT-treated cells, $p = 0.023$; for VEGFR1, $p < 0.001$; for VEGFR2, $p = 0.024$; VEGFR2 in DHT-treated cells, $p = 0.01$). Data are presented as average of three experiments. (*f*) Migration assay shows the effect of induced AR overexpression on the migratory ability of VCaP cells. Data are presented as average of three experiments (mean migrated pCMV control cells = 178, mean migrated pCMV-AR cells = 286, difference = 108, 95% CI = 257–314, $p = 0.004$). $p < 0.05$, as indicated by "*", $p < 0.01$, as indicated by "**". Androgen Receptor (Santa Cruz), MMP9 (ab38898, Abcam), VEGF (Upstate Biotechnology), VEGFR1 and VEGFR2 (Santa Cruz), alpha-Tubulin (Biosite), pAkt (Ser473, Cell Signaling and Biosite) and PIP5K1α (Protein Technologies) were used.

expression in vehicle control and in ISA-2011B-treated cells were 0.73 and 0.41, 95% CI = 0.40–0.41; difference = 0.32, $p < 0.001$) and VEGFR2 in VCaP cells (mean value of VEGFR2 expression in vehicle control and in ISA-2011B-treated cells were 0.75 and 0.64, 95% CI = 0.63–0.64; difference = 0.11, $p = 0.002$; Figs. 4*c* and 4*d*). The effect of inhibition of PIP5K1α on invasive behaviors of VCaP cells was further assessed. Blocking PIP5K1α by ISA-2011B remarkably reduced the migratory ability of VCaP cells ($p < 0.001$; Fig. 4*e*). Thus, our findings pinpoint the PIP5K1α/AKT as primary key players that control the signaling molecules that are associated with AR and MMP9/VEGF signaling axis in PCa cells. To determine

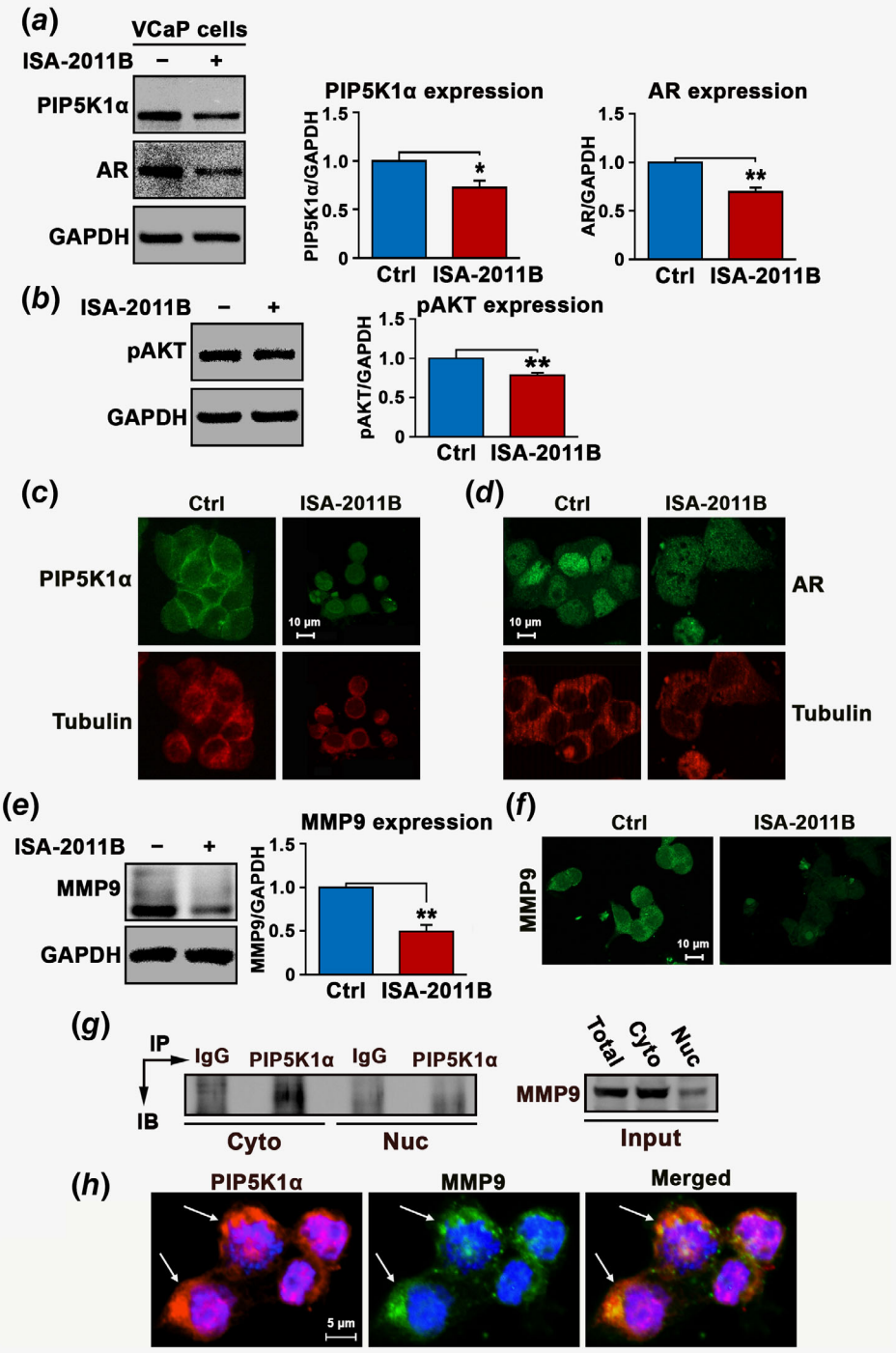

Figure 3. Legend on next page.

whether the regulation of PIP5K1α by AR might occur at transcriptional level, we examined effect of AR overexpression and DHT stimulation on mRNA expression of PIP5K1α using quantitative RT-PCR assay. Induced AR overexpression or DHT treatment did not have significant effect on PIP5K1α mRNA level (Fig. 4*f*). However, we found that AR and PIP5K1α formed immune-complexes in both cytosolic and nuclear compartments of VCaP cells as determined by immunoprecipitation assays (Fig. 4*g*). This suggests that AR rather influences PIP5K1α expression at protein level.

A direct functional link between MMP9 is mediated through PIP5K1α using PC-3 cells lacking AR

To further elucidate the precise interconnection among AR, PIP5K1α and MMP9 signaling pathways, we employed AR-negative cell line PC-3 cells. We examined the effect of induced AR in the absence or presence of DHT on PIP5K1α, pAKT and MMP9 signaling pathways in PC-3 cells (Figs. 5*a*, 5*c* and 5*e*). We observed that induction of exogenous AR significant increased expression of PIP5K1α and pAKT in PC-3 cells compared to the control (for PIP5K1α, $p = 0.03$; Fig. 5*b*, for pAKT, $p = 0.01$, Fig. 5*e*). Transfected-AR also increased MMP9 expression by threefold compared to the control (mean value of MMP9 expression in pCMV control cells and in pCMV-AR cells were 0.86 and 2.49, difference = 1.63, 95% CI = 2.14–2.85, $p = 0.048$, Fig. 5*c*). DHT stimulation of transfected AR had no significant effect on MMP9 expression ($p = 0.67$, Fig. 5*c*), indicating that AR is sufficient to affect MMP9 expression. Immunofluorescence analysis further revealed that the membrane and cytosol localization of MMP9 which was enhanced in PC-3 cells expressing pCMV-AR vector (Fig. 5*d*). Induction of exogenous AR also led to increased VEGF expression in PC-3 cells (mean value of VEGF expression in pCMV control cells and in pCMV-AR cells were 0.47 and 0.73, difference = 0.26, 95% CI = 0.7–0.76, $p = 0.04$, Figs. 5*c* and 5*e*). Similarly, Induced AR expression increased VEGFR1 and VEGFR2 ($p = 0.03$ *vs.* $p = 0.03$; Fig. 5*f*). This finding further validates a direct link between AR and MMP9/VEGF signaling axis.

To further investigate whether induced AR expression may increase the invasive phenotype of PC-3 cells, we employed tumor-spheroid invasion assays to mimic the *in vivo* tumor conditions. To this end, AR-transfected PC-3 cells or control PC-3 cells were firstly subjected to formation of tumor-spheroids at three-dimensions for 10 days. The equal amount of tumor-spheroids were then subjected to the migration assay. Interestingly, cancer cells were able to release themselves from the tumor-spheroids and migrate to the lower chamber. AR-transfected tumor cells displayed a remarkably increase in the migration rate by 2.4-fold compared to control ($p < 0.001$; Fig. 5*g*). Interestingly, tumor cells derived from tumor spheroids which were formed by AR-transfected cells and were stimulated with DHT showed a greater increase by 3.4-fold of that of control vector-transfected cells treated with DHT ($p = 0.014$, Fig. 5*g*). In contrast, ISA-2011B treatment led to a significant decrease in MMP9 expression coincident with a decreased expression in pAKT in control PC-3 cells (for MMP9, $p = 0.0012$, for pAKT, $p = 0.03$) or PC-3 expressing AR (for MMP9, $p = 0.043$, pAKT, $p < 0.001$; Fig. 5*h*).

The role of AR and MMP9 in regulate downstream target gene cyclin A1

It is known that the coregulators allow interaction of the AR complex with the transcription apparatus to stimulate target gene transcription.[26] To provide further mechanistic insights on the impact of MMP9 on AR transcriptional activity on its target gene in PCa cells, we utilized a cyclin A1 full-length promoter-luciferase reporter construct. We have previously shown that AR, VEGF and cyclin A1 promote PCa invasion and metastasis through feedback loops.[27] We cotransfected PC-3 cells with PCMV-AR or PCMV control vectors with the cyclin A1 promoter-luciferase reporter construct (cyclin A1-Luc) or control luciferase reporter (Luc) construct. AR increased remarkably the

Figure 3. Evaluation the functional link between AR, PIP5K1α and MMP9 in VCaP cells. (*a*, *b*) The effects of ISA-2011B on the expression of various proteins in VCaP cells. Immunoblots show the expression of PIP5K1α, AR and pAKT S473 (Mean value of PIP5K1α expression in vehicle-treated control cells and in ISA-2011B-treated cells were 0.88 and 0.61, difference = 0.27, 95% CI = 0.61–0.62, $p = 0.003$; Mean value of AR expression in vehicle-treated control cells and in ISA-2011B-treated cells were 0.69 and 0.47, 95% CI = 0.46–0.47; difference = 0.22, $p < 0.001$; Mean value of pAKT expression in vehicle-treated control cells and in ISA-2011B-treated cells were 1.11 and 0.87, difference = 0.25, 95% CI = 0.84–0.89, $p < 0.001$). Data are presented as average of two independent experiments. (*c*, *d*) Representative immunofluorescent images show the expression and subcellular localization of PIP5K1α and AR (in FITC) and tubulin (Alexa 546) in VCaP cells that were treated with vehicle control or ISA-2011B. (*e*) The effect of control and ISA-2011B treatment on VCaP cells. Immunoblots show the expression of MMP9 (Mean value of MMP9 expression in vehicle control and in ISA-2011B-treated cells were 2.32 and 1.23, difference = 1.09, 95% CI = 0.94–1.53; $p < 0.001$). (*f*). Representative immunofluorescent images show the expression and subcellular localization of MMP9 in VCaP cells that were treated with DMSO control and ISA-2011B. (*g*) VCaP cells were subjected to immunoprecipitation (IP) assay. Antibody against PIP5K1α was used to pull down its associated immunocomplexes in the membrane/cytoplasmic fractions *vs*. nuclear fractions of VCaP cells, and antibody to IgG was used as a negative control. Antibody against MMP9 was used for immunoblot analysis (IB). The equal amount of total lysates, cytoplasmic (Cyto) and nuclear (Nuc) fractions were used as input control for immunoblot analysis of the immunoprecpitated lysates. (*h*) Representative immunofluorescent images show the expression and subcellular localization of PIP5K1α (in red) and MMP9 (in green) in VCaP cells under confocal microscope. The colocalization of PIP5K1α and MMP9 (in orange) in the cytoplasmic compartment is indicated by the arrow in the merged image.

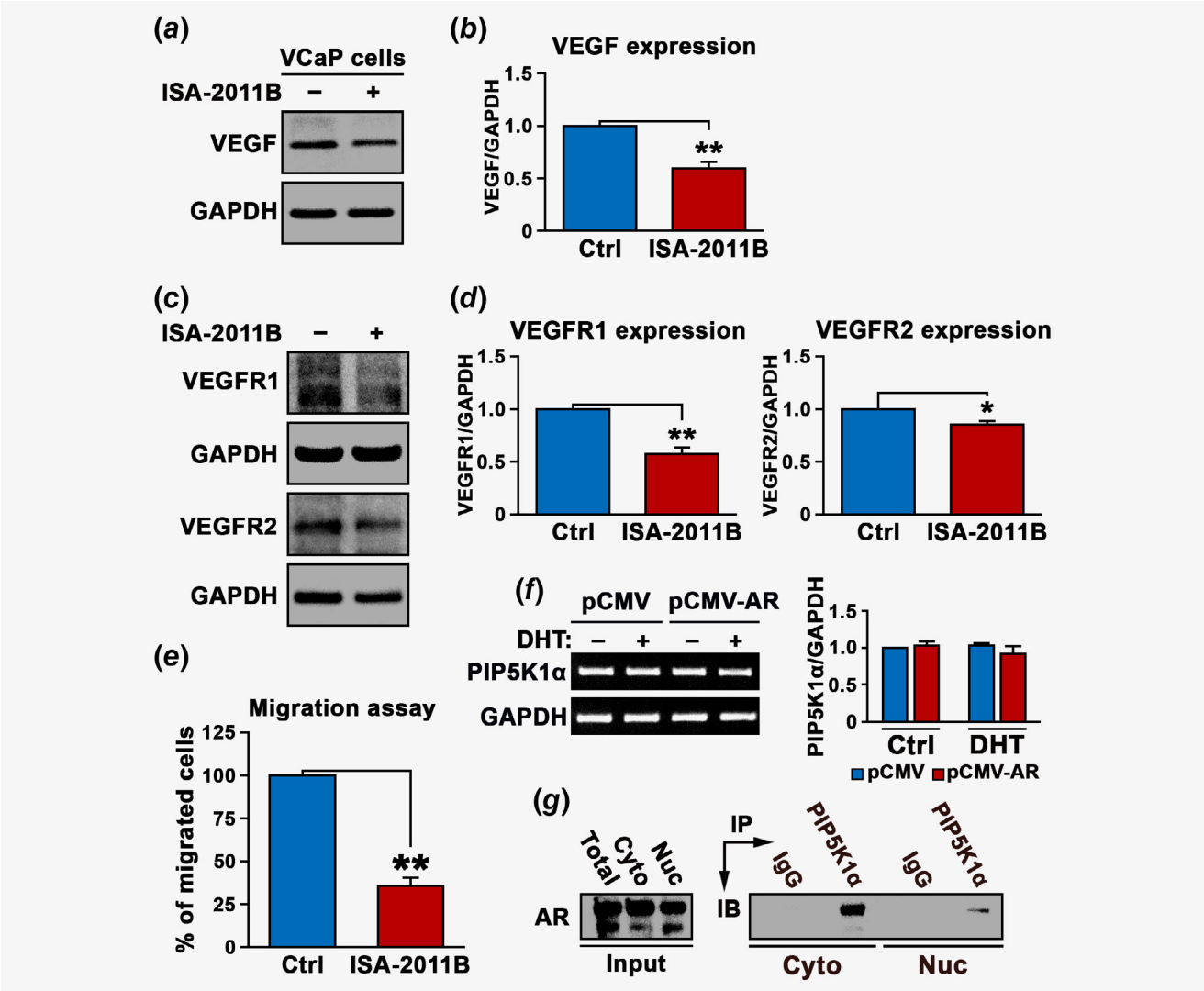

Figure 4. The functional effect of ISA-2011B on the angiogenic factors in VCaP cells. (*a–d*) The effect of ISA-2011B on VCaP cells. Immunoblots show the expression of VEGF, VEGFR1 and VEGFR2 in VCaP cells (Mean value of VEGF expression in vehicle control and in ISA-2011B-treated cells were 0.71 and 0.45, difference = 0.26, 95% CI = 0.42–0.47; $p < 0.001$; Mean value of VEGFR1 expression in vehicle control and in ISA-2011B-treated cells were 0.73 and 0.41, 95% CI = 0.40–0.41; difference = 0.32, $p < 0.001$; Mean value of VEGFR2 expression in vehicle control and in ISA-2011B-treated cells were 0.75 and 0.64, 95% CI = 0.63–0.64; difference = 0.11, $p = 0.002$). (*e*) Migration assays show the effect of ISA-2011B on the migratory ability of VCaP cells. Data are presented as average of two independent experiments (control treatment mean migrated cells = 192, ISA-2011B treatment mean migrated cells = 66, difference = 125, 95% CI = 56–77, $p < 0.001$). $p < 0.05$, as indicated by "*", $p < 0.01$, as indicated by "**". (*f*) Quantification of mRNA expression of PIP5K1α, normalized with GAPDH as determined by quantitative RT-PCR, in VCaP cells expressing control vector (pCMV) or AR (pCMV-AR) after treatment with DMSO (–) or DHT (+). (*g*) VCaP cells were subjected to immunoprecipitation (IP) assay. Antibody against PIP5K1α was used to pull down its associated immunocomplexes in the membrane/cytoplasmic fractions *vs.* nuclear fractions of VCaP cells, and antibody to IgG was used as a negative control. Antibody against AR was used for immunoblot analysis (IB). The equal amount of total lysates, cytoplasmic (Cyto) and nuclear (Nuc) fractions were used as input control for immunoblot analysis of the immunoprecipitated lysates.

cyclin A1-luciferase activity by approximately twofold as compared to that of control vector ($p = 0.009$; Fig. 6*a*). This suggests that AR is able to transactivate cyclin A1 transcriptional activity. Next, we examined whether induced MMP9 expression may enhance AR transcriptional activity on cyclin A1 promoter. Induced coexpression of MMP9 and AR remarkably increased cyclin A1 reporter luciferase activity as compared to that by AR alone ($p = 0.02$, Fig. 6*a*). This novel finding provides new evidence further supporting that AR and MMP9 are functionally associated with each other.

Functional consequence of induced MMP9 expression in PCa tumor-spheroids stimulated with myeloid cells in xenograft mouse model

To further gain mechanistic insights into the role of intracellular MMP9 and its downstream effectors in PCa cells, we

induced MMP9 overexpression by transfecting VCaP cells with pLX304-MMP9 or control vectors. Immunoblot analysis confirmed the MMP9 overexpression in VCaP cells as compared to the control ($p < 0.001$; Fig. 6*b*). Interestingly, induced overexpression of MMP9 had no significant effect on the expression of AR ($p = 0.47$; Fig. 6*b*), but led to a

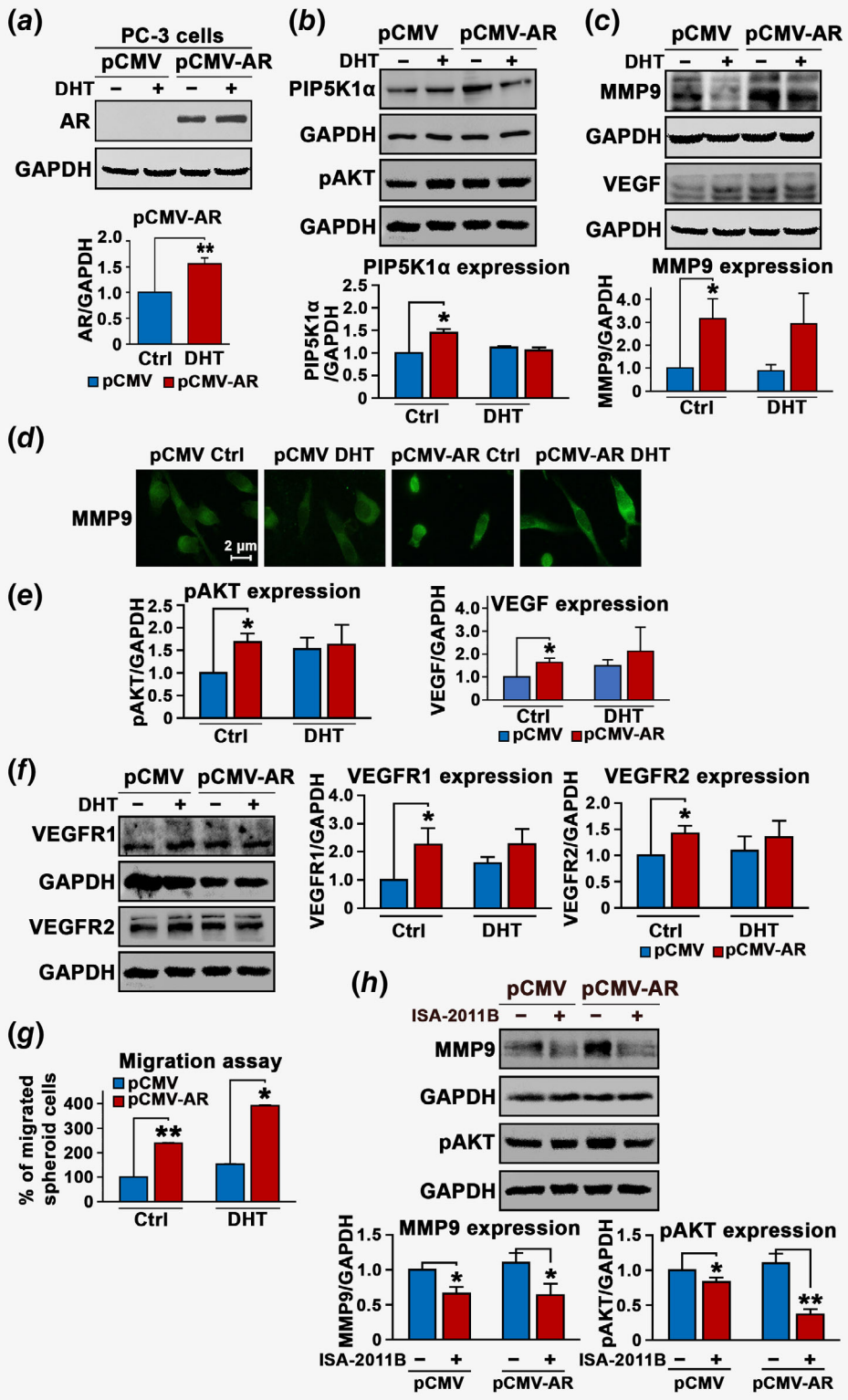

Figure 5. Legend on next page.

significant increase in VEGF expression ($p < 0.001$) and VEGFR2 ($p = 0.005$; Fig. 6*b*). MMP9 overexpression had no significant effect on VEGFR1 expression in VCaP cells ($p = 0.35$, Supporting Information Fig. S2). As expected, overexpression of MMP9 resulted in a significant increase in PIP5K1α ($p < 0.001$; Fig. 6*c*).

Since the proteolytic MMP9 function can be activated after tumor cells being stimulated by their associated myeloid cells within the microenvironment during cancer invasion and metastasis.[28] We prestimulated MMP9-transfected VCaP cells and control cells with U-937 cells, the myeloid cell line. We then subjected the cells to the tumor-spheroid formation assay. VCaP cells overexpressing MMP9 formed significantly higher numbers of tumor spheroids compared to controls ($p < 0.001$; Fig. 6*d*). Next, we implanted equal amount of tumor-spheroids derived from MMP9-transfected VCaP cells or control cells prestimulated by U-937 cells subcutaneously into the nude mice. Interestingly, the tumors from MMP9-overexpressing group appeared to be larger. Although the statistical significance was unable to be determined, it appeared that MMP9 group mice hade larger inflammatory signs around tumors (Fig. 6*e*).

Discussion

It is believed that AR is a key factor that promotes PCa progression and metastasis. However, the functional link between AR and the key proteins such as MMP9 and VEGF signaling axis that control PCa angiogenesis and metastasis remained largely unknown. In our study, we aimed to gain deeper understanding of the precise molecular mechanism and functional impact of AR, MMP9 and their associated PIP5K1α/pAKT and VEGF signaling in PCa. Our new findings illustrated the molecular mechanisms underlying the interplay of these key players in growth and invasion of PCa (Fig. 6*f*).

We observed that patients with elevated level of MMP9 mRNA suffered poorer DFS as compared to those with lower MMP9 expression level in their tumors, although this difference was not statistically significant. Both AR and MMP9 play important roles in promoting cancer cell invasion and metastatic dissemination to distant organs. We found that metastatic tumors had higher levels of AR and MMP9, and this suggests that patients had tumors expressing elevated levels of both AR and MMP9 may have high risk to experience cancer metastasis. MMP9 is one of the key factors which promote cancer metastasis and it is also a transcriptional target of AR, commonly present in metastatic PCa.

We showed that AR overexpression increased MMP9 protein level in AR-positive VCaP cells and AR-negative PC-3 cells. Also, AR overexpression significantly increased expression of PIP5K1α and phosphorylated AKT in PCa cells. This is in agreement with our previously reported studies suggesting that PIP5K1α and AR stabilize and enhance their protein expression by formation of protein–protein complexes with AR and CDK1.[10,13] Furthermore, AR-induced increase in MMP9 expression was mediated by PIP5K1α and phosphorylated AKT.

Thus, AR is sufficient to trigger the sequential activation of interconnected pathways including MMP9, PIP5K1α/AKT and VEGF signaling axis to promote PCa cell survival and invasion in an androgen-depleted environment by increasing the protein expression of AR. In addition, we showed that DHT enhanced the expression of AR without leading to an increase in protein expression of MMP9, PIP5K1α, pAKT and VEGF and VEFG2 in VCaP cells or PC-3 cells. Given that these proteins are the coactivators of AR, their expression may not be directly affected by DHT. Since the role of DHT as a ligand is to induce conformational change of AR leading to AR stabilization, binding to its coactivators, entering into the nucleus.[2,3]

The effect of induced AR overexpression on MMP9 protein expression was mediated through PIP5K1α *via* posttranscriptional mechanisms. PIP5K1α/AKT appeared to be an important pathway which can lead to MMP9 activation, and our

Figure 5. The functional link between AR and MMP9 and PIP5K1α/AKT and VEGF signaling axis. (*a*) Immunoblots show the expression of AR in control DMSO or DHT treated PC-3 cells expressing control (pCMV) or AR expressing vectors (pCMV-AR). (Mean value of AR expression in pCMV-AR cells and in DHT-treated pCMV-AR cells were 0.75 and 1.08, difference = 0.33, 95% CI = 0.99–1.16, $p < 0.001$.) (*b* and *e*) Immunoblots show the expression of PIP5K1α and pAKT in control DMSO or DHT-treated PC-3 cells expressing control (pCMV) or AR expressing vectors (pCMV-AR). (Mean value of PIP5K1α expression in pCMV control cells and in pCMV-AR cells were 0.73 and 1.10, difference = 0.37, 95% CI = 1.07–1.13, $p = 0.03$.) (*c* and *e*) Immunoblots show the expression of MMP9 and VEGF in control DMSO or DHT treated PC-3 cells ($p = 0.048$). Mean value of VEGF expression in pCMV control cells and in pCMV-AR cells were 0.47 and 0.73, difference = 0.26, 95% CI = 0.7–0.76, $p = 0.04$.). Data is presented as average of two independent experiments. $p < 0.05$, as indicated by "*", $p < 0.01$, as indicated by "**". (*d*) Representative immunofluorescent images show the expression and subcellular localization of MMP9 in PC-3 cells in DMSO treated or DHT treated PC-3 cells expressing control (pCMV) or AR expressing vectors (pCMV-AR). (*e*) Quantification of the immunoblots of pAKT and VEGF as shown in (*b* and *c*) from at least two independent experiments is shown. $p < 0.05$, as indicated by "*". (*f*) Immunoblots show the effect of control DMSO or DHT treatment on VEGFR1 and VEGFR2 in PC-3 cells expressing control (pCMV) or AR expressing vectors (pCMV-AR). Data are presented as average of two independent experiments. $p < 0.05$, as indicated by "*", $p < 0.01$, as indicated by "**". (*g*) Migration assays show the migratory ability of tumor cells of tumor-spheroids derived from DMSO treated or DHT treated PC-3 cells expressing control (pCMV) or AR expressing vectors (pCMV-AR). (pCMV control *vs*. pCMV-AR control $p < 0.001$, pCMV DHT *vs*. pCMV-AR DHT $p = 0.014$). Data are presented as average of two independent experiments $p < 0.05$, as indicated by "*", $p < 0.01$, as indicated by "**". (*h*) Immunoblots show the effect of control DMSO or ISA-2011B treatment on MMP and pAKT in PC-3 cells expressing control (pCMV) or AR expressing vectors (pCMV-AR). Data are presented as average of two independent experiments $p < 0.05$, as indicated by "*", $p < 0.01$, as indicated by "**".

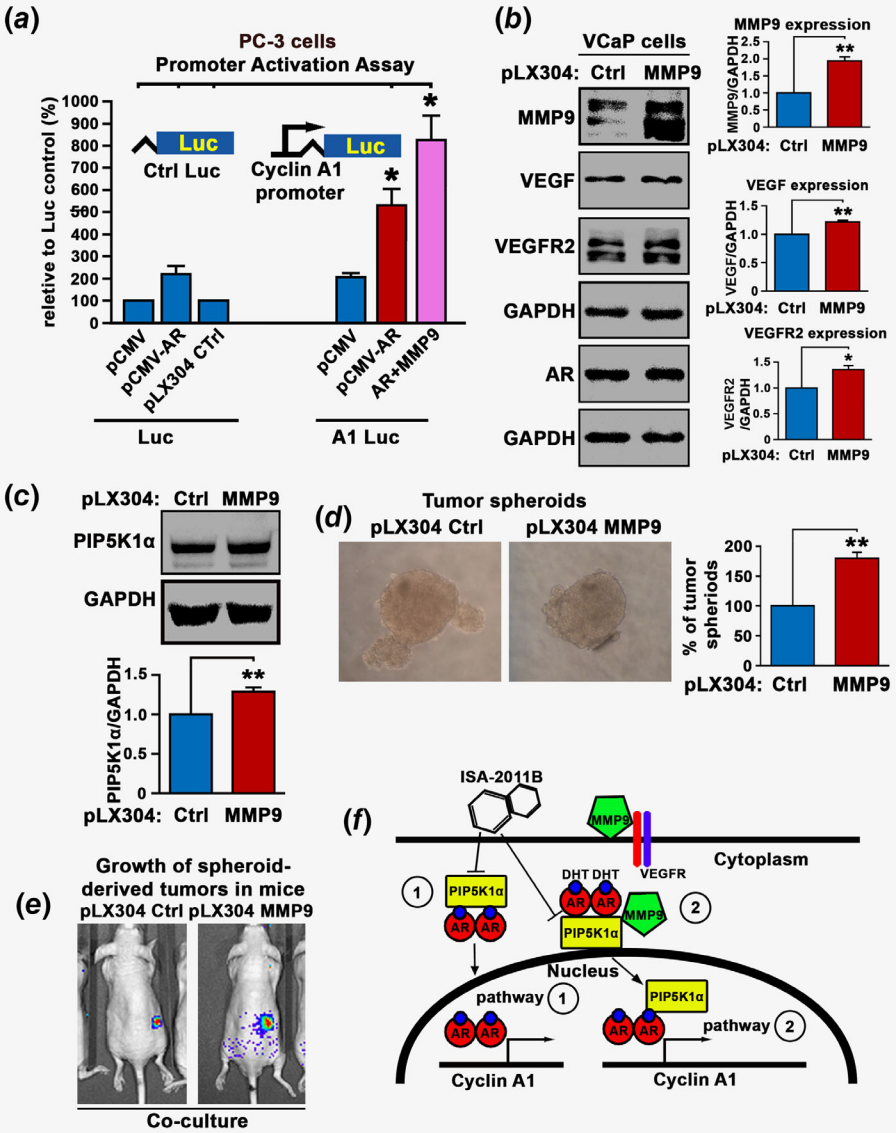

Figure 6. Functional impact of AR, MMP9 and PIP5K1α in *in vitro* tumor-spheroid formation and in tumor growth in xenograft mouse model. (*a*) Effect of induced AR alone or together with induced MMP9 expression on the activity of full-length cyclin A1 promoter was assessed using luciferase assay. The vectors were induced together with luc-reporter vector "Luc" or cyclin A1 promoter-luc reporter vector "A1 Luc" into PC-3 cells. (*b*) Immunoblots show the expression of MMP9, AR, VEGF and VEGFR2, in VCaP cells expressing control (pLX304) or pLX304-MMP9 vector. The quantifications of the immunoblots from two independent experiments are shown in the right panel (Mean value of MMP9 expression in PLX304 control cells and in pLX304-MMP9 cells were 1.18 and 2.2, difference = 1.03, 95% CI = 1.97–2.43, $p < 0.001$; Mean value of VEGF expression in PLX control cells and in pLX-MMP9 cells were 0.61 and 0.75, difference = 0.14, 95% CI = 0.72–0.77, $p < 0.001$; Mean value of VEGFR2 expression in PLX control cells and in pLX-MMP9 cells were 0.96 and 1.29, difference = 0.33, 95% CI = 1.25–1.33, $p = 0.005$). Data are presented as average of two independent experiments $p < 0.05$, as indicated by "*", $p < 0.01$, as indicated by "**". (*c*) Immunoblots show the expression of PIP5K1α in control (pLX) or pLX-MMP9 cells. Mean value of PIP5K1α expression in PLX control cells and in pLX-MMP9 cells were 0.55 and 0.71, difference = 0.16, 95% CI = 0.71–0.72; $p < 0.001$). Data presented as average of two independent experiments. $p < 0.05$, as indicated by "*", $p < 0.01$, as indicated by "**". (*d*)The effect of MMP9 overexpression on the ability of VCaP cells to form tumor-spheroids. VCaP cells expressing control (pLX304) or pLX304-MMP9 vectors were subjected to tumor-spheroid formation assays. *Y*-axis shows the spheroid counts. Data are presented as average of four experiments (pLX304-CTR mean number of spheroids = 42, pLX304-MMP9 mean number of spheroids = 75, difference = 33, 95% CI = 67–83, $p < 0.001$). $p < 0.05$, as indicated by "*", $p < 0.01$, as indicated by "**". (*e*) Representative imaging of xenograft mice bearing tumors expressing luciferase-reporter gene is shown. VCaP cells expressing control (pLX304-CTR) or pLX304-MMP9 vectors were prestimulated with U-937 cells and were subjected to tumor-spheroids formation. The tumor-spheroids from each group were subcutaneously implanted into nude mice. (*f*) Schematic model depicts two possible pathways that involve in AR/PIP5K1α/MMP9 in activation of downstream target gene cyclin A1 during progression of PCa. Pathway 1 as indicated as #1 shows that enhanced AR induced by PIP5K1α in response to DHT stimulation enter into the nucleus and activates the target gene (cyclin A1) transcription. Alternative pathway, pathway 2 as indicated shows that MMP9 enhance AR forms complex with PIP5K1α, which is in turn in complexes with MMP9. Increased AR expression also leads to increased PIP5K1α and MMP9 expression. MMP9 increases PIP5K1α expression leading to the enhanced AR transcriptional activity on its target gene (cyclin A1).

findings on that PIP5K1α forms protein–protein complexes with MMP9, which further suggests that MMP9 may directly acts as mediator of signal transduction in the cytosol.

It has been shown that MMP9 is associated with EGFR/PI3K/AKT pathways in PCa.[19] In our study, we have identified MMP9 and PIP5K1α as important cofactors for AR, which play important roles in enhancing AR transcriptional activity on its target gene, cyclin A1. The elevated sequential activation of AR/PIP5K1α/AKT/MMP9/VEGF signaling axis contributed to increased invasiveness and growth of metastatic tumors. Conversely, treatment with PIP5K1α inhibitor significantly suppressed invasiveness of PCa cells expressing constitutively activated AR, coincident with its inhibitory effect on AR/MMP9/VEGF pathways. Further studies are needed to understand the precise mechanism that mediates the effect of AR/PIP5K1α on MMP9 expression during PCa metastasis.

Our new finding is in agreement with our previous studies in xenograft mice,[10,13] and further provides evidence suggesting that ISA-2011B exerts its effect on cooperative mechanisms involving AR, MMP9 and PIP5K1α/AKT pathways which drive PCa growth and invasion. Our findings provide new information to guide the targeted therapy for treatment of invasive castration-resistant PCa.

Acknowledgements

This work was supported by grants from the Swedish Cancer Society, The Swedish Children Foundation, H2020-MSCA-ITN-2018-European Commission, Malmö Cancer Foundation, the Government Health Innovation Grant, Kempe STF, Umeå University, Medical Faculty Grants Norland fund for Cancer Forskning, Umeå University and Medical Faculty Grants to JLP. The Grants from University of Copenhagen to NØ. The Royal Physiographical Foundation to MS. We sincerely thank Pirkko Härkönen (University of Turku, Turku) and Yvonne Lundberg Giwercman (Lund University, Lund) for providing reagents for our study. We also thank Kristina Ekström-Holka for technical help.

References

1. Chen CD, Welsbie DS, Tran C, et al. Molecular determinants of resistance to antiandrogen therapy. *Nat Med* 2004;10:33–9.
2. Feldman BJ, Feldman D. The development of androgen-independent prostate cancer. *Nat Rev Cancer* 2001;1:34–45.
3. Takeda DY, Spisak S, Seo JH, et al. A somatically acquired enhancer of the androgen receptor is a noncoding driver in advanced prostate cancer. *Cell* 2018;174:422–32.e13.
4. Viswanathan SR, Ha G, Hoff AM, et al. Structural alterations driving castration-resistant prostate cancer revealed by linked-read genome sequencing. *Cell* 2018;174:433–47. e19.
5. Grasso CS, Wu Y-M, Robinson DR, et al. The mutational landscape of lethal castration-resistant prostate cancer. *Nature* 2012;487:239–43.
6. Loijens JC, Anderson RA. Type I phosphatidylinositol-4-phosphate 5-kinases are distinct members of this novel lipid kinase family. *J Biol Chem* 1996;271:32937–43.
7. van den Bout I, Divecha N. PIP5K-driven PtdIns (4,5)P2 synthesis: regulation and cellular functions. *J Cell Sci* 2009;122:3837–50.
8. Shaw RJ, Cantley LC. Ras, PI(3)K and mTOR signalling controls tumour cell growth. *Nature* 2006; 441:424–30.
9. Janku F, Yap TA, Meric-Bernstam F. Targeting the PI3K pathway in cancer: are we making headway? *Nat Rev Clin Oncol* 2018;15:273–91.
10. Semenas J, Hedblom A, Miftakhova RR, et al. The role of PI3K/AKT-related PIP5K1alpha and the discovery of its selective inhibitor for treatment of advanced prostate cancer. *Proc Natl Acad Sci USA* 2014;111:E3689–98.
11. Waugh MG. Amplification of chromosome 1q genes encoding the Phosphoinositide signalling enzymes PI4KB, AKT3, PIP5K1A and PI3KC2B in breast cancer. *J Cancer* 2014;5: 790–6.
12. Sarwar M, Syed Khaja AS, Aleskandarany M, et al. The role of PIP5K1alpha/pAKT and targeted inhibition of growth of subtypes of breast cancer using PIP5K1alpha inhibitor. *Oncogene* 2019;38: 375–89.
13. Sarwar M, Semenas J, Miftakhova R, et al. Targeted suppression of AR-V7 using PIP5K1alpha inhibitor overcomes enzalutamide resistance in prostate cancer cells. *Oncotarget* 2016;7:63065–81.
14. Heissig B, Hattori K, Dias S, et al. Recruitment of stem and progenitor cells from the bone marrow niche requires MMP9 mediated release of kit-ligand. *Cell* 2002;109:625–37.
15. Comamala M, Pinard M, Theriault C, et al. Downregulation of cell surface CA125/MUC16 induces epithelial-to-mesenchymal transition and restores EGFR signalling in NIH:OVCAR3 ovarian carcinoma cells. *Br J Cancer* 2011;104: 989–99.
16. Elbaz M, Nasser MW, Ravi J, et al. Modulation of the tumor microenvironment and inhibition of EGF/EGFR pathway: novel anti-tumor mechanisms of Cannabidiol in breast cancer. *Mol Oncol* 2015;9:906–19.
17. Garrido P, Shalaby A, Walsh EM, et al. Impact of inducible nitric oxide synthase (iNOS) expression on triple negative breast cancer outcome and activation of EGFR and ERK signaling pathways. *Oncotarget* 2017;8:80568–88.
18. Pei J, Lou Y, Zhong R, et al. MMP9 activation triggered by epidermal growth factor induced FoxO1 nuclear exclusion in non-small cell lung cancer. *Tumour Biol* 2014;35:6673–8.
19. Mandel A, Larsson P, Sarwar M, et al. The interplay between AR, EGF receptor and MMP9 signaling pathways in invasive prostate cancer. *Mol Med* 2018;24:34.
20. Aalinkeel R, Nair BB, Reynolds JL, et al. Overexpression of MMP9 contributes to invasiveness of prostate cancer cell line LNCaP. *Immunol Invest* 2011;40:447–64.
21. Bergers G, Brekken R, McMahon G, et al. Matrix metalloproteinase-9 triggers the angiogenic switch during carcinogenesis. *Nat Cell Biol* 2000; 2:737–44.
22. Kessenbrock K, Plaks V, Werb Z. Matrix metalloproteinases: regulators of the tumor microenvironment. *Cell* 2010;141:52–67.
23. Ravindranathan P, Lee TK, Yang L, et al. Peptidomimetic targeting of critical androgen receptor-coregulator interactions in prostate cancer. *Nat Commun* 2013;4:1923.
24. Miftakhova R, Hedblom A, Semenas J, et al. Cyclin A1 and P450 aromatase promote metastatic homing and growth of stem-like prostate cancer cells in the bone marrow. *Cancer Res* 2016;76:2453–64.
25. Taylor BS, Schultz N, Hieronymus H, et al. Integrative genomic profiling of human prostate cancer. *Cancer Cell* 2010;18:11–22.
26. Tan MH, Li J, Xu HE, et al. Androgen receptor: structure, role in prostate cancer and drug discovery. *Acta Pharmacol Sin* 2015;36:3–23.
27. Wegiel B, Bjartell A, Tuomela J, et al. Multiple cellular mechanisms related to cyclin A1 in prostate cancer invasion and metastasis. *J Natl Cancer Inst* 2008;100:1022–36.
28. Andersson P, Yang Y, Hosaka K, et al. Molecular mechanisms of IL-33-mediated stromal interactions in cancer metastasis. *JCI Insight* 2018;3:e122375.